

Bundle Description of Packing and Dynamics in Polycarbonate Homopolymers, Copolymers, and Blends

Jon M. Goetz,[†] Jinhua Wu,[‡] Albert F. Yee,[‡] and Jacob Schaefer^{*,†}

Department of Chemistry, Washington University, St. Louis, Missouri 63130, and Department of Materials Science and Engineering, The University of Michigan, Ann Arbor, Michigan 48109

Received August 1, 1997; Revised Manuscript Received February 2, 1998

ABSTRACT: Dipolar-rotational spin-echo ^{13}C NMR spectra at 15.1 MHz have been obtained for 12 homopolymers, copolymers, and blends of polycarbonate, poly(ether carbonate), poly(ether sulfone), dimethyl polycarbonate, and tetramethyl polycarbonate. The spectra were used to determine the fraction of nonmethylated phenylene rings that are blocked from undergoing π flips faster than 10 kHz at 300 K. This fraction is interpreted in terms of a simple two-chain bundle packing model in which empirically determined steric parameters specify the interchain interactions between flexible chain linkers and rigid chain extenders. The success of this bundle description suggests that the glassy state for all of these polycarbonate-like systems has local mainchain orientational order.

Interchain internuclear distances measured by solid-state NMR experiments on Bisphenol A polycarbonate have been interpreted recently in terms of a bundle model of the glassy state.¹ The most important features of this model for polycarbonate include (i) dense packing, (ii) local mainchain orientational order, (iii) a tight distribution of interchain spacings, and (iv) a carbonyl carbon to quaternary carbon, nearest-neighbor interchain distance of about 6 Å for each repeat unit. The NMR-determined interchain distances have also been used as constraints on energy-minimized molecular dynamics simulations of the phenylene-ring dynamics within a polycarbonate bundle.² These simulations have emphasized the importance for each polycarbonate chain of the packing of its single nearest-neighbor chain. In this paper we present the results of phenylene-ring dynamics NMR experiments performed on a variety of polycarbonate homopolymers, copolymers, and homogeneous blends. The results are interpreted in terms of the few specific, interchain steric interactions that result from the pairwise chain packing of the Whitney–Yaris model. This interpretation supports the notion that a bundle model for packing is applicable to a variety of polycarbonate-like glassy polymers, all characterized by alternating rigid and flexible repeat units in the main chain.

Experiments

Synthesis of Dimethyl Polycarbonate (D). (4-Hydroxyphenyl)-2-propanol was produced by the reaction of 4-bromophenol with *n*-butyllithium at -78°C , followed by the addition of acetone. This material was reacted with 2,6-dimethylphenol using HCl(g) as catalyst to produce dimethyl Bisphenol A, which was then converted into the corresponding bis(chloroformate) using phosgene, *N,N*-dimethylaniline, and (dimethylamino)pyridine. Finally, dimethyl polycarbonate (D) was synthesized from dimethyl Bisphenol A and its bis(chloroformate) following the general procedure for polycarbonate synthesis previously described.^{3,4}

Synthesis of OB, OT, and OBOT Polycarbonate Copolymers. Copolymerization of 4,4'-oxydiphenol with Bisphenol A bis(chloroformate), or with tetramethyl Bisphenol A

bis(chloroformate), produced the alternating polycarbonate copolymers OB and OT, respectively. To generate a strictly alternating sequence of O, with B and T, oligomer OBO was synthesized using the same method as described for B_x oligomers.⁵ This was followed by copolymerization of OBO oligomer with tetramethyl Bisphenol A bis(chloroformate) to form OBOT copolymer.

Preparation of Blends. Homogeneous blends⁶ of (i) one part polycarbonate (B) and one part tetramethyl polycarbonate (T) (with the blend designated B + T), (ii) one part [ring-3,3'- $^{13}\text{C}_2$]polycarbonate and 19 parts perdeuterated T (B + 19T), (iii) one part BT and six parts perdeuterated B (BT + 6B), and (iv) one part BT and six parts T (BT + 6T) were made by precipitation from chloroform into methanol.⁷

Sample Preparation for Dynamic Mechanical Spectroscopy. Solution cast films were used in the DMS measurements. Experimental procedures for the DMS tests are described in detail elsewhere.³

NMR. ^{13}C NMR spectra were obtained at room temperature at 15.1 MHz using a 12-in. resistive magnet and a home-built spectrometer details of which have been described previously.⁸ The single, 11-mm diameter, radio frequency coil was connected by a low-loss transmission line to a double-resonance tuning circuit. A 1-kW ENI LPI-10H amplifier was used for the ^1H channel and an ENI A-300 amplifier for the ^{13}C channel. Cross-polarization transfers were performed at 50 kHz, carbon π pulses at 50 kHz, and proton dipolar decoupling at 100 kHz. Rotors with 600-mg sample capacities were made from plastic (Kel-F) and supported at both ends by air-pumped journal bearings. In these experiments, a 350-mg powder sample was positioned in the center of the rotor by Kel-F spacers.

DRSE. Carbon dipolar line shapes were characterized by dipolar rotational spin-echo (DRSE) ^{13}C NMR with dipolar evolution over one rotor cycle.⁸ This is a two-dimensional experiment in which, during the additional time dimension, carbon magnetization is allowed to evolve under the influence of ^1H – ^{13}C coupling, while ^1H – ^1H coupling is suppressed by homonuclear multiple-pulse semiwindowless MREV-8 decoupling.⁹ DRSE is well-suited to the examination of dipolar couplings in unlabeled materials. The cycle time for the homonuclear decoupling pulse sequence was 33.6 μs , resulting in decoupling of proton–proton interactions as large as 60 kHz. Sixteen MREV-8 cycles fit exactly into one rotor period with magic-angle spinning at 1859 Hz. A 16-point Fourier transform of the time dependence of the intensity of any peak resolved by magic-angle spinning yields a 16-point dipolar frequency spectrum, scaled by the MREV-8 decoupling and broken up into sidebands by the spinning. Broad dipolar

[†] Washington University.

[‡] The University of Michigan.

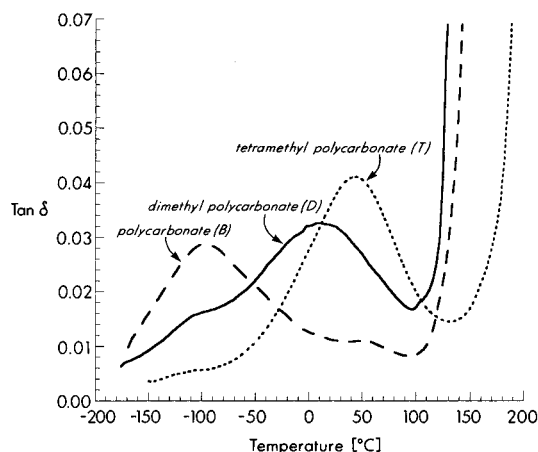


Figure 1. Dynamic mechanical spectra at 1 Hz of polycarbonate (B), dimethyl polycarbonate (D), and tetramethyl polycarbonate (T).

powder spectra (called Pake patterns) appear for carbons with strong ^1H – ^{13}C coupling, with narrower patterns observed for carbons with weaker couplings. Because the second spinning sideband is near the maximum of a rigid-lattice dipolar Pake powder pattern under the conditions of our experiments,⁸ the ratio of intensities of the second to first dipolar sidebands (n_2/n_1) is a sensitive measure of averaging of the phenylene-ring ^1H – ^{13}C dipolar coupling by molecular motion. This ratio changes from about 1.3 in the absence of motion to 0.5 in the presence of large-amplitude motions such as ring flips. For example, for the protonated aromatic-carbon peak of the static ring of polycrystalline dimethoxybenzene,¹⁰ we observed an n_2/n_1 of 1.33, and for the corresponding peak of polycarbonate, a value of 0.45. The n_2/n_1 intensity ratio is also about 0.5 for a methyl carbon directly bonded to three protons which are undergoing rapid rotations about the methyl carbon C_3 axis. The DRSE experiment was calibrated by matching the calculated C–H dipolar sideband spectrum (with a room-temperature MREV-8 scale factor¹¹ of 0.39) for polycrystalline 1,4-dimethoxybenzene.

Results

Dimethyl Polycarbonate. Even though the basic architecture of B, D, and T polycarbonates is the same, the mechanical response of each is distinctly different. For example, the low-temperature loss peak of B is shifted by 150 K for T (Figure 1). The DMS of D shows intermediate behavior to that of B and T, which indicates that some but not all of the cooperative mainchain motions of B that change the shape or volume of the glassy matrix under stress are inhibited by the presence of just two ring methyl groups.^{2,4} Part of the width of the sub- T_g loss peak for D is due to structural heterogeneity. Depending on the regiospecificity of the addition of the bis(chloroformates) of dimethyl Bisphenol A and Bisphenol A, carbonate linkages in D may be flanked by zero, two, or four aromatic methyl groups.

The chemical-shift ^{13}C NMR spectrum of D is indistinguishable from the spectra of the compositionally equivalent B + T blend and BT copolymer (see Figures 1 and 4 of ref 5). However, the time-domain dipolar evolutions in DRSE experiments have differences. The 120 ppm line of D (which arises from protonated aromatic carbons of nonmethylated rings) is completely dephased after 4 MREV-8 cycles (Figure 2), while those of B + T and BT are not.⁵ Following Fourier analysis, the n_2/n_1 ratio of the dipolar sideband spectrum of the 120 ppm line is 0.73 for D (Table 1), compared to 0.45

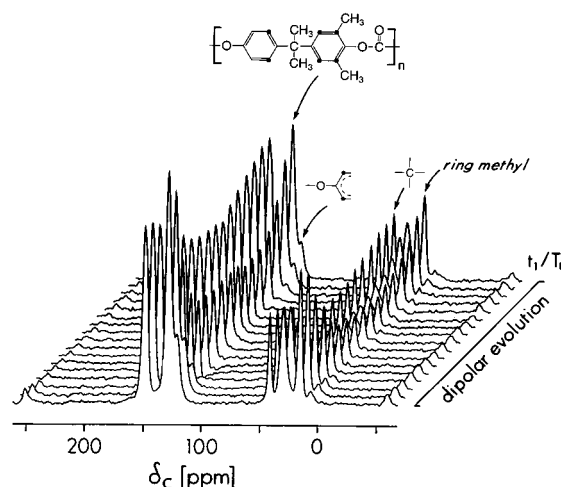


Figure 2. Dipolar rotational spin-echo 15.1-MHz ^{13}C NMR spectra of dimethyl polycarbonate (D) as a function of ^1H – ^{13}C dipolar evolution time during which proton–proton interactions are suppressed by multipulse decoupling. Chemical shifts were measured in ppm from external tetramethylsilane. The dipolar evolution times vary from zero to one rotor period. Magic-angle spinning was at 1859 Hz.

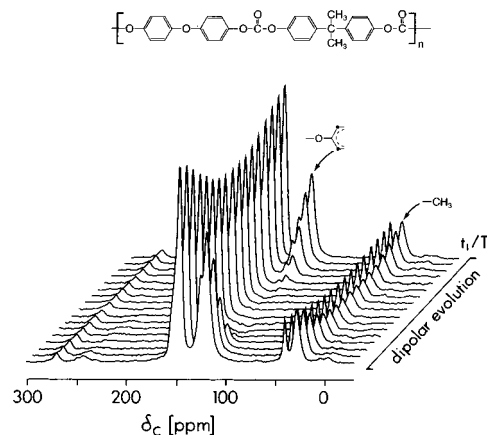


Figure 3. Dipolar rotational spin-echo ^{13}C NMR spectra of the alternating copolymer (OB) made by joining the repeat units from poly(ether carbonate) and polycarbonate. The dipolar evolution times vary from zero to one rotor period. Magic-angle spinning was at 1859 Hz.

for B + T, and 0.55 for BT (Table 2, last column). The relative intensities of the centerband and first four dipolar sideband intensities for the 128 ppm lines of D and T are comparable (Table 1), suggesting similar ring dynamics. Direct quantitative conclusions are complicated by the fact that the 128 ppm lines for both D and T arise from a mix of protonated and nonprotonated aromatic carbons. The n_2/n_1 ratios for the 15 ppm ring-methyl carbon peaks of both D and T were also the same; both values are 0.43 ± 0.03 .

Polycarbonate Copolymers. The 120 ppm line for OB is due to carbons in both O and B rings in the repeat unit (Figure 3). The DRSE dephasing of this line is slower than for the corresponding line in D (Figure 2). About one-fourth of the OB intensity is left after four MREV-8 cycles and the n_2/n_1 ratio is 0.54 (Table 2). None of the T ring-carbons contribute to the 120 ppm line in DRSE spectra of the mixed copolymer OBOT (Figure 4). The dephasing rate and n_2/n_1 ratio for the protonated-aromatic 120 ppm line of OBOT are intermediate to those of D and OB (Figures 2–4 and Table 2). Protonated aromatic-carbon sideband intensity ra-

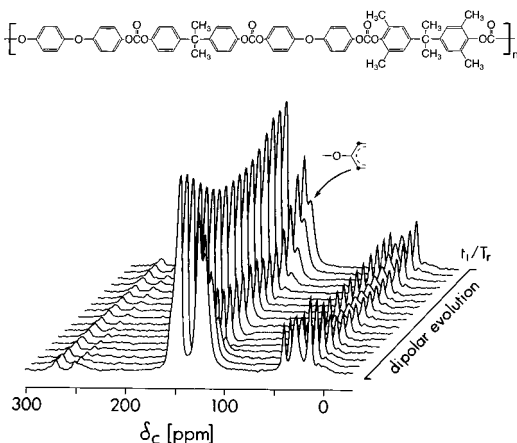


Figure 4. Dipolar rotational spin-echo ^{13}C NMR spectra of the alternating copolymer (OBOT) made by joining the repeat units from poly(ether carbonate), polycarbonate, and tetramethyl polycarbonate. The dipolar evolution times vary from zero to one rotor period. Magic-angle spinning was at 1859 Hz.

Table 1. Dipolar Sideband Intensities for Aromatic Carbon Signals of Dimethyl Polycarbonate (D) and Tetramethyl Polycarbonate (T)

polymer	centerband or sideband number ^a				
	0	1	2	3	4
T (obsd, 128 ppm)	5.68	1.00	0.72	0.28	0.13
D (obsd, 120 ppm)	1.25	1.00	0.73	0.27	0.13
D (obsd, 128 ppm)	4.16	1.00	0.76	0.27	0.11
D (calcd, 128 ppm) ^b	4.21	1.00	0.73	0.28	0.13

^a Using 0–16 MREV-8 cycles in one rotor period with magic-angle spinning at 1859 Hz. Estimated accuracy (based on signal-to-noise ratios) is ± 0.02 . ^b From $1/3$ D (obs, 120 ppm) + $2/3$ T (obs, 128 ppm).

Table 2. Phenylene-Ring Dynamics for Homopolymers, Copolymers, and Blends of Polycarbonate (B), Poly(ether carbonate) (O), Dimethyl Polycarbonate (D), and Tetramethyl Polycarbonate (T)

polymer	sequence ^a	fraction of nonflipping rings ^b		dipolar sideband ratio (n_2/n_1) ^{b,d}
		predicted ^c	obsd	
B	R L	0	0	0.45
O	r l	$1/3$	0.38 ^e	0.77
D	R L	$1/3$	0.33	0.73
T	R L			
BT	R L R L	$1/6$	0.12	0.55 ^f
OB	r l r l	$1/6$	0.11	0.54
OT	r l R L	$1/3$	0.29	0.70
OBOT	r l r l r l R L	$2/9$	0.21	0.63
B plus T	R l plus L R	0	0	0.45 ^f
B plus 19T	R l plus L R	0	0.06	0.50
BT plus 6B	R L R L plus l R	0	0.01	0.46
BT plus 6T	R L R L plus L R	$1/4$	0.22	0.64 ^f

^a From Table 3 and Figure 6. ^b Nonmethylated phenylene rings only. ^c From experimental n_2/n_1 and parameters of Table 3. ^d From the 120 ppm protonated aromatic carbon line using 0–16 MREV-8 cycles in one rotor period with magic-angle spinning at 1859 Hz. Estimated accuracy (based on signal-to-noise ratios) is ± 0.02 . ^e For poly(ether sulfone). ^f Reference 5.

tios for all of the copolymers examined by DRSE are presented in Table 2. The copolymer methyl-carbon n_2/n_1 ratios were all 0.43 ± 0.03 .

Polycarbonate Blends. The DRSE evolution of the 120 ppm line arising from the ^{13}C label in B + 19T is not obscured by the 130 ppm T peak (insert, Figure 5). Natural-abundance ^{13}C contributions to the spectra were suppressed by perdeuteration of T and by the use of a short ^1H – ^{13}C cross-polarization transfer time. The

[Aromatic- ^{13}C]B + 19 [Perdeuterated]T

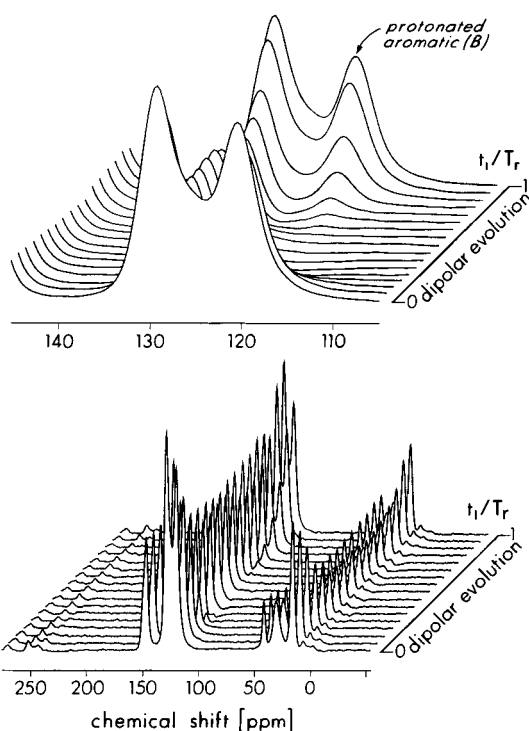


Figure 5. Dipolar rotational spin-echo ^{13}C NMR spectra of the homogeneous blend of one part of [ring-3,3'- $^{13}\text{C}_2$]B and 19 parts of perdeuterated T. The dipolar evolution times vary from zero to one rotor period. Magic-angle spinning was at 1859 Hz.

n_2/n_1 dipolar sideband ratio for the 120 ppm peak is 0.50, slightly greater than the corresponding observed ratio for the B + T blend (Table 2). For the BT copolymer, replacing nearest-neighbor BT chains with (perdeuterated) B chains has only a minor effect on the 120 ppm n_2/n_1 ratio for the protonated-aromatic carbons of B units in BT (BT + 6B, Table 2), whereas replacing BT chains with T chains has a more substantial effect on this ratio (BT + 6T, Table 2).

Discussion

Fractions of Flipping Nonmethylated Rings. In polycarbonate, the protonated aromatic-carbon dipolar sideband n_2/n_1 ratio is 0.45. This value is mostly, but not exclusively, the result⁶ of the averaging of the ^1H – ^{13}C dipolar coupling by ring-flip rates greater than about 10 kHz at 300 K. In the absence of large-amplitude motional averaging, n_2/n_1 is 1.3. We determine the fraction, f , of B phenylene rings that are flipping in polycarbonate copolymers and blends from $(n_2/n_1)_{\text{obsd}} = 0.45f + 1.3(1 - f)$, where the observed sideband ratio corresponds to the 120 ppm aromatic carbon peak, which arises exclusively from B units. Because the observed ratios are all close to $1/2$ (Table 2), most of the B rings are flipping, even in copolymers with high concentrations of T. The fraction of B rings not flipping, $1 - f$, is reported in Table 2, and ranges from a low of zero to a high of 0.38 for commercial poly(ether sulfone). About one-third of the nonmethylated rings in D are not flipping (Table 2), and none of the methylated rings. The latter conclusion is based on the match of observed and calculated dipolar sideband intensities for the 128 ppm line of D (Table 1). The calculated intensities were

obtained using the nonflipping rings of T as a standard. In addition, the n_2/n_1 ratio of 0.43 for the 15 ppm ring-methyl line of D shows no signs of motional averaging due to flips of methylated rings. This is also true for methylated rings in the DRSE spectra of T or any T-containing copolymer.⁵

The Whitney–Yaris Model for Ring Flips in Polycarbonate. Whitney and Yaris² have developed a generalized Langevin dynamics simulation of motion for a model of pure polycarbonate and have suggested a possibility for the mechanism of the ring-flipping process. A phenylene-ring π flip occurs when there is an increase of about 0.5 Å in the separation between the center of a ring and that of the closest ring of the nearest-neighbor chain. This separation must be accompanied by an increase in the rotational kinetic energy of the ring attempting the flip. In the Whitney–Yaris model, the π -flip gate in polycarbonate results from the synchronization of the arrival of a lattice phonon with a reduction in an intermolecular steric barrier.

Because of the structural similarity and miscibility^{3,6} of B, O, D, T, and most of their combinations, it seems reasonable to suppose that the Whitney–Yaris model is applicable to the blends and copolymers of Table 2, as well as to B itself. Within the framework of the Whitney–Yaris model, no T ring or methylated D ring can ever flip because the 0.5-Å reductions in inter-ring separations do not lower the barriers sufficiently for 180° rotations of methyl-substituted rings.¹² Thus, the methyl-substituted rings are prevented from flipping by an intermolecular packing interaction, not an intramolecular steric barrier. This result is consistent with solution-state NMR experiments which show that even for chloro-substituted polycarbonate rings, full rotation occurs in solution with a correlation time of the order of a nsec.¹³ Furthermore, no B ring in a B + T blend is ever constrained from flipping because a 20° rotation about the T-ring C_2 axis (such ring fluctuations are always present)² is sufficient to move the methyl group out of the way of a flipping B ring. On the other hand, it is plausible that the increased stiffness of B units near T units in BT would be sufficient to enable a proximate T ring to block a B-ring flip, at least in a fraction of sites in the glass.⁵ The increased stiffness of the BT main chain results from increased interchain steric hindrance of ring methyls and not from a change in flexibility of the carbonate linkage. By this interpretation, the 12% fraction of nonflipping B rings in BT (Table 2) is due to the most densely packed regions in the glass. These B rings are in parts of chains that are stiffened by interchain interactions of two methylated rings. (See Figure 6 in ref 5.) The stiffened chain has a reduced ability to rearrange cooperatively with its neighbors and so provide the 0.5-Å dilation needed for a B ring to flip. Thus, a nonflipping ring is blocked by a combination of interchain steric interactions.

Phenomenological Description of Packing and Ring-Flip Dynamics. To extend the physical arguments of the Whitney–Yaris model to all the polymers of Table 2, we represent those elements that the main chains have in common by the partial structures of Figure 6. Each chain can be described (Table 2, second column) in terms of a sequence of alternating rigid extenders (r, R, \mathcal{R}) and flexible linkers (l, L, \angle). An unambiguous sequence is defined by the full structure of the repeat unit, but a full structure is not defined

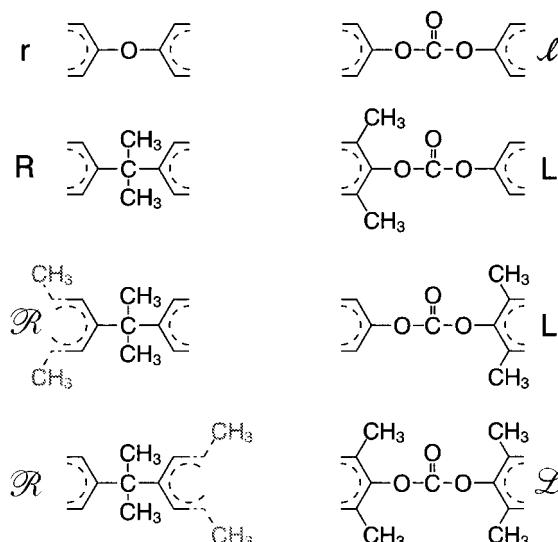


Figure 6. Structural elements common to polycarbonate-like homopolymers and copolymers. Each element consists of a central extender (r, R, \mathcal{R}) or a central carbonate linker (l, L, \angle), each surrounded by half-aromatic rings. An unambiguous sequence of structural elements is defined by the full structure of the repeat unit (see second column of Table 2), even though a full structure is not defined by a sequence because the symbols L and \mathcal{R} are each used for more than one partial structure. The suppressed lettering of the \mathcal{R} unit indicates that at least one of the two possible ring positions on the half aromatic ring of the adjacent structural element must be occupied by a methyl group to distinguish \mathcal{R} from R.

Table 3. Chain-Packing Interaction Parameters for Polycarbonates

flexible\rigid	\mathcal{R}	R	r
\angle	1	0	
L	$1/3$	0	$1/3$
l	0	0	$1/3$

by a sequence because the symbols L and \mathcal{R} are each used for more than one partial structure. We could remove the ambiguity by defining two versions of L and \mathcal{R} , but that would introduce unnecessary interchain packing interactions (cf. below). For the purposes of this discussion, we always know the structure of the polymer (Table 2, first column) and are interested only in writing a sequence for the polymer in terms of common structural elements. The motivation for writing these sequences is to identify the kinds of interchain steric interactions that result from the pairwise chain packing of the Whitney–Yaris model. For example, the nearest-neighbor chain in polycarbonate (B) that gates ring flips always packs so that rigid extenders (R) and flexible linkers (l) are opposite one another.² Thus, the single important interchain steric interaction in polycarbonate packing is R–l. Because no phenylene rings are blocked from flipping in polycarbonate, for purposes of deciding on the fraction of nonflipping rings, we define the relative R–l steric interaction as zero (Table 3).

We take the relative steric interaction for \mathcal{R} –L as $1/3$, based on the observed fraction (Table 2) of nonflipping rings in dimethyl polycarbonate (D). The fact that few B rings are blocked in homogeneous blends of polycarbonate and tetramethyl polycarbonate (B + 19T) means that the \mathcal{R} –l and R– \angle parameters are both close to zero. If these parameters are zero, then the intermediate R–L interaction must be zero as well. The r–L and r–l parameters are each $1/3$ as established by the fractions of nonflipping rings for OT and OB copolymers, respectively, reported in Table 2. The \mathcal{R} – \angle parameter

we designate as one, but this interaction is not important for us because no phenylene rings with a 120 ppm signal are involved. The r - \angle interaction does not occur for any of the polymers of Table 2. Thus, all the relevant chain-packing interactions for Table 2 are established from just five experimental determinations of n_2/n_1 using B and D homopolymers, OB and OT copolymers, and the B + 19T blend. A possible physical interpretation of these parameters is that proximal ring methyls potentially stiffen the chain by an interchain steric interaction⁵ which increases in the order l to L to \angle . At the same time, proximal rings (with or without methyls) interfere with one another to a greater extent around the ether linkage (r) than around the isopropylidene unit (R) because of tighter packing unobstructed by side chain methyls. More quantitative insights await detailed molecular modeling.

We can use the simple chain-packing parameters of Table 3 to decide on the fraction of nonflipping rings for the five remaining polymers of Table 2 that were not part of the parametrization. For example, the alternating copolymer BT has two nonmethylated phenylene rings per repeat unit. The sequence for BT is ... $R\ L\ \angle\ L\ \dots$ which means that there are only two types of interchain steric interactions (R - L and L - \angle) needed to describe the packing of a repeat unit of a BT chain with its interchain nearest neighbor. Within the context of the model, these two chains form a rudimentary bundle. The nonmethylated ring of the R unit of the ... $R\ L\ \angle\ L\ \dots$ repeat sequence is not blocked by an interchain L (R - L interaction parameter of zero, Table 3). However, the nonmethylated ring of the L unit (which is a less flexible linker than that in polycarbonate homopolymer) is potentially blocked if the nearest neighbor is \angle (L - \angle interaction parameter of $1/3$, Table 3). We assume that there is no discrimination in packing flexible linkers next to rigid extenders and each possibility is equally likely. Thus, the fraction of blocked nonmethylated rings is $1/2 \times 1/3 = 1/6 = 0.16$, which is close to the experimental value of 0.12. Obviously, a better match to experiment could be made if the L - \angle interaction parameter were assumed to be $1/4$ instead of the $1/3$ of Table 3. In fact, a value of $1/4$ was reported for the L - \angle interaction parameter, based on the compositional dependence of the fraction of nonflipping rings in B_xT copolymers.⁵ Nevertheless, we will retain the simplicity of Table 3 for now and avoid the complications of a multiparameter description. Thus,

only two interaction parameters are needed (0 and $1/3$; the R - \angle parameter is not used) to describe the 11 n_2/n_1 ratios of Table 2.

Calculations for O, OBOT, B + T, BT + 6B, and BT + 6T polymers, copolymers, and blends were done following the BT example, by enumerating all the possible nearest-neighbor, linker-extender, and interchain interactions and estimating contributions to ring blocking by using the interaction parameters of Table 3. We substituted poly(ether sulfone) for poly(ether carbonate) in the determination of flipping rings in O because our version of poly(ether carbonate) was low molecular weight and partially crystalline. All of the predicted and observed fractions of blocked rings are in reasonable agreement (Table 2). We take this agreement as an indication of the general applicability of a Whitney-Yaris bundle model to the polycarbonate-like systems of Table 2. By implication, the polycarbonate packing model of Hutnik et al.¹⁴ is not applicable to these systems because the chain-packing parameters of Table 3 infer local order and specific proximities, both of which are absent in a random packing model.

Acknowledgment. This work was supported by NSF Grant DMR-9729734.

References and Notes

- (1) Klug, C. A.; Zhu, W.; Tasaki, K.; Schaefer, J. *Macromolecules* **1997**, *30*, 1734.
- (2) Whitney, D.; Yaris, R. *Macromolecules* **1997**, *30*, 1741.
- (3) Jho, J. Y.; Yee, A. F. *Macromolecules* **1991**, *24*, 1905.
- (4) Xiao, C.; Yee, A. F. *Macromolecules* **1992**, *25*, 6800.
- (5) Klug, C. A.; Wu, J.; Xiao, C.; Yee, A. F.; Schaefer, J. *Macromolecules* **1997**, *30*, 6302.
- (6) Fischer, E. W.; Hellmann, G. P.; Spiess, H. W.; Hörth, F. J.; Ecarius, U.; Wehrle, M. *Makromol. Chem. Suppl.* **1985**, *12*, 189.
- (7) Schmidt, A.; Kowalewski, T.; Schaefer, J. *Macromolecules* **1993**, *26*, 1729.
- (8) Schaefer, J.; Stejskal, E. O.; McKay, R. A.; Dixon, W. T. *Macromolecules* **1984**, *17*, 1479.
- (9) Rhim, W. K.; Elleman, D. D.; Vaughan, R. W. *J. Chem. Phys.* **1973**, *59*, 3740.
- (10) Garbow, J. R.; Schaefer, J. *Macromolecules* **1987**, *20*, 819.
- (11) Schaefer, J.; McKay, R. A.; Stejskal, E. O.; Dixon, W. T. *J. Magn. Reson.* **1983**, *52*, 123.
- (12) Whitney, D.; Yaris, R. private communication.
- (13) O'Gara, J. F.; Desjardins, S. G.; Jones, A. A. *Macromolecules* **1981**, *14*, 64.
- (14) Hutnik, M.; Gentile, F. T.; Ludovice, P. J.; Suter, U. W.; Argon, A. S. *Macromolecules* **1991**, *24*, 5962.

MA9711699